1. Introduction: Outline - "Focusing on why we care about stratospheric aerosol in background conditions and what have past studies told us"

The existence of persistent atmospheric aerosol after volcanic eruptions must have been apparent to careful atmospheric observers from early times. The reddish diffraction ring around the sun following large volcanic eruptions was first carefully described by Sereno Bishop nine days after the eruption of Krakatoa, in late August 1883, and lead to the name Bishop's ring. Less certain is that early observers suspected that aerosol persisted in the stratosphere during volcanically quiescent periods. The first published report suggesting a persistent aerosol layer in the stratosphere used purple twilight observations [Gruner and Kleinert, 1927]. Quantitative observations characterizing the altitudes, sizes, masses, and aerosol compositions involved were first provided by balloonborne impactor measurements in the late 1950s [Junge et al., 1961]. Subsequent measurements by both aircraft- and balloon-borne impactors suggested the global distribution of stratospheric aerosol [Junge and Manson, 1961; Chagnon and Junge, 1961]. On a few occasions, in addition to the impactors which measured particles > 0.1 μm, Aitken particle counters were included on the balloon gondola. While the Aitken nuclei concentration decreased through the stratosphere, particles > 0.1 μm had a maximum in concentration near 20 km, suggesting an aerosol source in this region [Junge et al., 1961]. These particles were large enough to create the purple twilight noted by early observers.

Junge et al.'s measurements were at the end of an extended volcanic-free period [Stothers, 1996], but did not establish a baseline for stratospheric aerosol. Quantifying the global stratospheric aerosol burden, and describing the role of volcanic eruptions, required long term measurements which began in the early 1970s using lidar [Jäger, 1991; Osborn et al., 1995; DeFoor et al., 1992]; balloonborne particle counters [Hofmann et al., 1975; Hofmann and Rosen, 1980; Hofmann, 1990]; and in the late 1970s satellite instruments: SAM (Stratospheric Aerosol Measurements) II (1979-1991) [Pepin *et al.*, 1977; Poole and Pitts, 1994], SAGE (1979-1981) (Stratospheric Aerosol and Gas Experiment) and SAGE II (1984-present) [McCormick *et al.*, 1979]. The impact of sulfur rich volcanic eruptions then became obvious and these have been the dominant source of stratospheric aerosol for the past 30 years. Within the last century the most recent 30 year period has been a relatively active volcanic period. Sato et al. [1993] and Stothers [1996], using solar and stellar extinction data, show that the previous 120 years was dominated by eight major eruptions. Four of these occurred between 1880 and 1910 and four since 1960. The long term measurements which began in the 1970s, have captured the complete cycle for three major eruptions with a global stratospheric impact: Fuego (14°N, October 1974, 3-6 MT), El Chichón (17°N, April 1982, 12 MT) and Pinatubo (15°N, June 1991, 30 MT) [McCormick et al., 1995]. Within this record there have been four volcanically quiescent periods, 1974, 1979, 1989-1990, and 1997 - 2003.

Stratospheric aerosol are important for a number of processes which affect the chemical and radiation balance of the atmosphere [McCormick et al., 1995; Solomon, 1999]. During periods of high volcanic aerosol load there is evidence for heterogeneous chemistry on the sulfate aerosol reducing ozone [Angell et al., 1985; Hofmann and Solomon, 1989; Jäger and Wege, 1990; Gleason et al., 1993; Deshler et al., 1996], for stratospheric warming [Labitzke and McCormick, 1992; Angell, 1993; Russell et al.,

1993], and for tropospheric cooling [Manabe and Wetherald; Pollack et al., 1976; 1967; Dutton and Christy, 1992; Hanson et al., 1992]. During volcanically quiescent periods, when stratospheric aerosol is in a "background" state unperturbed by volcanism, radiative effects of stratospheric aerosol are negligible but these aerosol still play a role in the budget of several trace gases, in particular NO_x. NO_2 columns were reduced after both El Chichón and Pinatubo [Johnston and McKenzie, 1989; Johnston et al., 1992] from the hydrolysis of N_2O_5 on water bearing volcanic sulfuric acid aerosol [Rowland et al., 1986; Tolbert et al., 1988; Mozurkiewicz and Calvert, 1988]. At low aerosol loading NO_x increases and induces ozone loss from the nitrogen catalytic cycle [Crutzen, 1970]. Fahey et al. [1993] provided direct measurements of the anticorrelation of aerosol surface area and the NO_x/NO_y ratio. The hydrolysis of N_2O_5 saturates as aerosol surface area increases above 5-10 μm^2 cm^{-3}, thus the role aerosol play in controlling NO_x is primarily important during periods of low aerosol loading [Prather, 1992]. Changes in NO_x also affects the abundance of ClO_x and HO_x, both of which also react with ozone [Wennberg et al., 1994; Solomon et al., 1996]. The importance of aerosol in stratospheric chemistry first became apparent with the suggestion of its role in polar ozone loss [Solomon et al., 1986]. Long term stratospheric aerosol measurements had their beginnings about fifteen years prior to this realization.

The primary emphasis of long term stratospheric aerosol measurements has been on volcanic events. This is partly due to the significant impact large eruptions have on the stratosphere, to the increased signal they provide for instruments, to the dynamic nature of eruptions and their aftermath, to their global distribution, and to the fact that volcanic eruptions have dominated the signal for 20 of the past 30 years [Deshler et al., 2003]. In addition these eruptions are important for analyzing the short-term regional and global effects on climate of enhanced aerosol loading. This analysis is important for climate models, as aerosols can play an important role in influencing the long-term consequences of changing trace gas concentrations in the atmosphere. This chapter, however, is concerned with long-term non-volcanic stratospheric aerosol levels. Thus the emphasis shall be on levels present during years between major eruptions, rather than on temporary enhancements due to the eruptions themselves. Stratospheric aerosol during non-volcanic periods is referred to as background aerosol. This background aerosol level will be subject to various periodic perturbations, such as seasonal cycles, and long-term secular changes that govern the overall trend in the record. Identifying secular drifts in the background aerosol is crucial if we are to predict future aerosol levels.

We define background stratospheric aerosol to be that aerosol which remains in the stratosphere after all effects of perturbing volcanic eruptions have disappeared. It is anticipated that natural and anthropogenic emissions of sulfur, in the form of OCS and SO_2, will then be sufficient to maintain a population of stratospheric aerosol in quasi-steady state. Thus during background periods stratospheric aerosol measurements are expected to display a mean with a temporal gradient which, at a minimum, exceeds volcanic decay time scales, e.g. 3-4 years. During background periods measurements will remain within variations expected due to measurement error and non-volcanic geophysical oscillations, such as induced by changes in season or the quasi-biennial oscillation (QBO). A further complication results from primarily the use of instruments sensitive to bulk aerosol quantities, such as extinction or backscatter, for long term

measurements. Thus fine scale changes in aerosol size distribution may be difficult to observe, and our sensitivity is limited to the precision of the individual measurements.

The importance of possible changes in background stratospheric aerosol levels lead to the analysis of each quiescent period as it appeared in the record. The first of these analyses [Hofmann and Rosen, 1980; Hofmann and Rosen, 1981; Sedlacek et al., 1983] compared the pre-Fuego and pre-El Chichón periods.. Comparison of pre-El Chichón measurements with initial measurements of Junge et al. [1961] which were at the end of an extensive volcanic-free period suggested a possible increase of about of factor of five in aerosol concentration at 20 km during the intervening 20 years leading Hofmann and Rosen [1980] to suggest an increase of 9% yr^{-1} in aerosol mixing ratio at 0.15 μm particle radius. Sedlacek et al. [1983], comparing globally distributed airborne filter samples during 1974 and 1979, pre Fuego and pre El Chichón, suggested a 6% yr^{-1} increase in background stratospheric sulfur mass. This problem was revisited prior to Pinatubo. Hofmann [1990] compared measurements of aerosol mixing ratio for 0.15 and 0.25 μm radius thresholds during volcanically unperturbed periods in 1974, 1979, and 1989. No change was observed in the mixing ratio of 0.15 μm particles; however, there was a 50% increase in aerosol mixing ratio for particles > 0.25 μm between 1979 and 1989. Based on these changes Hofmann estimated an increase in aerosol mass on the order of 5% yr^{-1} over the decade which is consistent with the earlier estimates of Hofmann and Rosen [1980] and Sedlacek et al. [1983]. A similar increase in SAGE II extinction measurements over the same time period was observed; however, Thomason et al. [1997] suggested that 1989 may not have been at true background, due primarily to Nevado del Ruiz, Columbia, in 1985. Thus they suggested the elevated aerosol was due to residual volcanic effects.

Resolution of the questions raised by these studies had to wait for the third background period in the modern record, the present post Pinatubo period. Based on long term lidar measurements at Mauna Loa, Hawaii, Barnes and Hofmann [1997] suggest that the decay of aerosol loading following El Chichón and Pinatubo was influenced by the phase of the QBO in tropical stratospheric winds, that integrated aerosol backscatter in 1995 was below any previous observation at Mauna Loa. Hayashida and Horikawa [2001] used SAGE II extinction measurements to derive Ångström parameters and concluded that the pre-Pinatubo period was still influenced by volcanic eruptions from the mid 1980s and cannot be considered a real background period. Barnes and Hofmann [2001] used the present background period, extending from 1996, to demonstrate variability correlated with the phase of the QBO, with implications for the source of background stratospheric aerosol. Deshler et al. [2003] presented a thirty year record of mid latitude in situ measurements which suggest that stratospheric aerosol in the present, post-Pinatubo, period is at or below any previous background period. Thus these initial analyses of the post-Pinatubo aerosol suggest, in contrast to studies of earlier background periods, no long term increase in stratospheric background aerosol. This chapter will look closely at that conclusion.

2. Fundamental measurements - Outline - "1) measurements which can be used to compare volcanically quiescent periods. Each instrument subject to the usual questions - What are the measurement uncertainties (precision/accuracy)? How does measurement uncertainty change with aerosol loading? What changes in instrumentation have

occurred? What steps are used to insure data continuity, i.e. changes in calibration, changes in data screening, changes in protocol? What are the sampling/averaging intervals? Has the measurement focus shifted over the past 30 years? 2) Supplementary measurements which can be used to extend the record earlier? a) Junge's initial measurements (1960s) - these have been addressed by Hofmann and Rosen 1980, see below. b) Ground based passive extinction, e.g. photometers, pyroheliometers, these have not been addressed."

The purpose of this chapter is to compare stratospheric aerosol during the four volcanically quiescent periods in the modern aerosol record. To do this requires records which span at least two of these periods. This limits the measurements to the six longest records of stratospheric aerosol available. These are: 1) In situ aerosol concentration measurements at 0.15 and 0.25 μm radius from Laramie, Wyoming, USA (1971-2002, 41°N). Remote lidar backscatter measurements from: 2) São José dos Campos, Brazil (1972-2001, 23°S), 3) Mauna Loa, Hawaii, USA (1974-2002, 20°N), 4) Hampton, Virginia, USA (1974-2002, 37°N), 5) Garmisch-Partenkirchen, Germany (1976-2002, 48°N); and 6) Remote satellite extinction measurements from SAM II (1978-1994) and SAGE II (1984-2002). For each of these measurement platforms the fundamental measurements will be described and then compared during the volcanically quiescent periods, taking into account instrumental or operational changes in the measurements.

a) In situ measurements

Stratospheric aerosol measurements at Laramie, Wyoming, began in 1971 using an optical particle counter (OPC) initially developed by Rosen [1964]. The instrument, a white light counter measuring aerosol scattering at 25° in the forward direction, is a single particle counter, using Mie theory to determine aerosol size. An incandescent lamp, optics, and light controller supply a stable image of the incandescent lamp filament in the scattering region which is larger than the aerosol sample stream, thus edge effects are not a problem in defining sample volume. Light scattered from single particles passing through the beam is collected over a solid angle of ~ 30° and focused onto a photomultiplier tube (PMT) for pulse height detection. Two symmetrical independent photon paths limit noise, Rayleigh scatter, and the influence of cosmic rays by coincidence counting. Single coincident PMT pulses which exceed preset voltage levels are counted and used to determine aerosol concentration and size. Initial measurements in the 1970s consisted of measurements of particles > 0.15 and 0.25 μm at a sample flow rate of 1 liter min^{-1} [Pinnick and Hofmann, 1973; Hofmann et al., 1975].

In 1989 the OPC was modified to make measurements for particles > 0.4 μm, to increase the number of sizes measured, and to decrease the minimum concentration measurable. This was done to use the instrument to measure polar stratospheric cloud particles > 0.4 μm because of the importance of these particles in polar ozone loss [Solomon et al., 1986]. The scattering angle of the detector axis was increased from 25 to 40° and the air sample flow rate increased from 1 to 10 liter min^{-1}, with appropriate changes in inlet design to maintain roughly isokinetic sampling. This new scattering

angle allowed unambiguous detection of particles throughout the size range 0.15 - 10.0 μm in twelve size bins. Minimum detectable concentrations for the new OPC are 6 x 10⁻⁴ cm⁻³ as opposed to 6 x 10⁻³ cm⁻³ for the initial OPC. The new OPCs were first used in Antarctica in September 1989 [Hofmann and Deshler, 1991]. After calibration flights in Laramie to insure that the measurements at 0.15 and 0.25 μm radius are the same, within measurement limits, for the counter with scattering angle at 25 and 40°, the new OPC has replaced the old OPC for regular flights in Laramie [Deshler et al., 1993; Deshler et al., 2003].

Measurements with the new OPC from Laramie began in 1991; however tests with the original OPC continued until 1994 comprising 22 comparison flights. Current measurement capabilities consist of condensation nuclei (CN, r > 0.01 μm) and optically detectable aerosol, r ≥ 0.15 - 2.0 or 10.0 μm in twelve size ranges, from the surface to 30 km. These measurements can be inverted into a size distribution, but for the purposes of this work we will concentrate on the two fundamental measurements which span the past 30 years, the concentration of particles with r ≥ 0.15, 0.25 μm. These capture the vertical profile and amplitude of the layer first observed by Junge et al. [1961]. Additional details concerning the instrument function and laboratory tests are provided by Deshler et al., [2003].

Before each flight an OPC is calibrated by adjusting instrument gain until measured instrument response is consistent with theoretical instrument response for measurements on well characterized monodisperse aerosol. Instruments are calibrated using commercially available polystyrene latex spheres near 0.5 μm radius, a standard aerosol which has been used since the 1970s. It is sufficient to calibrate the instrument using only one particle size; however, the theoretical counter response curve has been checked a number of times using monodisperse particles of several sizes and compositions (refractive indices) [Pinnick et al., 1973; Zhao, 1996; Miao, 2001; Deshler et al., 2003].

Aerosol sizing errors result primarily from pulse broadening by PMTs for a constant optical input. Variations in intensity of the light beam, and in aerosol paths through the beam play a secondary role. These errors lead to sizing errors which are a function of index of refraction since the shape of the counter response curve varies with index of refraction. For temperatures above -65°C and water vapor concentrations near 5 ppmv, the real part of refractive index for sulfuric acid aerosol varies from 1.43 to 1.45, with no absorption [Steele and Hamill, 1981; Russell and Hamill, 1984]. Variations of index of refraction in this range lead to sizing errors well below those associated with pulse broadening, and do not contribute significantly. Using a nominal index of refraction of 1.45, counter response curves from Pinnick and Hofmann [1973] and Deshler et al. [2003], and the measured pulse broadening from PMTs leads to a sizing error of ± 10% at 0.15 and 0.25 μm.

Errors in concentrations measured by these instruments depends on variations in air sample flow rate, the reproducibility of a measurement from two identical instruments, and Poisson counting statistics. The pumps used for these instruments are constant volume gear displacement pumps. In laboratory tests pump flow rates are found to decrease by 3% at ambient pressures of 30 mbar and by 13% at 5 mbar [Miao, 2001]. These variations are, however, less than other uncertainties, and concentration measurements are not corrected for measurements at low pressures. Laboratory tests with two identical counters on several samples of differently sized monodisperse aerosol

indicate a measurement precision of $\pm$ 10% for relatively high concentrations of aerosol when Poisson counting statistics are not a factor.

Poisson counting statistics define the fractional uncertainty of a count as its inverse square root, $C^{-0.5}$ for C counts in one sample, becoming important at low concentrations. The aerosol concentration $N = C \, S / F$ for sample frequency, S, and flow rate, F. Thus the Poisson error fraction, in terms of concentration, is $(N \, F / S)^{-0.5}$. For these instruments: S = 0.1 Hz, F = 16.7 cm^3 s^{-1} for the old OPC, and F = 167 cm^3 s^{-1} for the new OPC. In the stratosphere these ambient air flow rates are reduced to about 80% of these values by temperature differences between outside air and pump. This leads to uncertainties of 85, 25, and 8% for concentrations of 0.01, 0.1, and 1.0 cm^{-3} at the low flow rate and concentrations of 0.001, 0.01, 0.1 cm^{-3} at the high flow rate. Poisson counting errors dominate at concentrations below 0.1 (0.01) cm^{-3} for the low (high) flow rate instrument. At concentrations higher than these a concentration error of $\pm$10% reflects measurement precision.

b) Remote lidar measurements

The first lidar (light detection and ranging) measurements of stratospheric aerosol were completed shortly after Junge et al.'s initial measurements [Fiocco and Grams, 1964]. Lidars provide remote vertically resolved measurements of atmospheric backscatter at one or more wavelengths. Lidar sites investigating stratospheric aerosols now range in latitude from 90°S to 80°N, with a number of sites in northern midlatitudes, and a few stations in the subtropics and southern midlatitudes. The standard measurement from any lidar is backscatter which is the fraction of the incident light intensity returned at 180° to the incident light pulse. The backscatter is presented as fraction per steradian per meter of scattering medium. In the atmosphere the backscatter arises from both molecular (Rayleigh) and aerosol scattering (Mie scattering in case of spherical particles). To obtain aerosol profiles from a lidar requires accounting for three factors which affect the backscattered light received by the lidar telescope, two way light extinction, molecular backscatter, and instrument normalization [e.g. Russell and Hake, 1977]. Molecular backscatter and extinction is typically calculated from pressure/temperature profiles provided by a nearby radiosonde station. In an aerosol free atmosphere and with a perfectly calibrated lidar this would coincide with the lidar backscattering measured.

Aerosol and ozone within the light path will diminish the strength of a returned lidar signal. To account for this effect requires a priori information on the ozone content of the atmosphere to calculate ozone extinction of the light beam for the two way path. Ozone profiles are obtained with either nearby ozone profile measurements or model atmospheres. Accounting for aerosol extinction is a bit more difficult since such profiles also represent one focus of the measurements, usually leading to an iterative correction procedure. Typically aerosol models are used to calculate aerosol extinction [Russell et al., 1981; Rosen and Hofmann, 1986]. The in situ Laramie data have provided the most comprehensive time dependent models of the ratio of aerosol extinction to backscatter. Using these data Jäger and Hofmann [1991] and Jäger and Deshler [2002] provide an assessment of the height resolved backscatter to extinction ratio for midlatitudes covering the period 1979 - 1999.

To remove molecular scatter from the lidar measurements use is made of the backscatter ratio, $R = (\beta_m + \beta_a)/\beta_m$, where β_m is molecular backscatter coefficient and β_a is aerosol backscatter coefficient. $\beta_m + \beta_a$ is the quantity measured, while β_m is calculated from the molecular density profile. Aerosol backscatter is then $\beta_a = (R-1) \beta_m$.

Normalization allows the lidar to be calibrated to the atmosphere. This is done after measurements are completed by selecting aerosol free regions in the atmosphere and then scaling the backscattering received from these regions to Rayleigh backscatter calculated from the molecular density profile. This scaling factor accounts for instrument characteristics for each lidar and for variations in instrument function over the integration periods. During volcanically quiescent periods an altitude for normalization can be found just above the tropopause where aerosol are often at a minimum, or can be found above 25 km. During volcanically active periods the region near the tropopause becomes contaminated with aerosol and it is necessary to extend the normalization region to altitudes above the aerosol layer, > 30 km.

Aside from uncertainties introduced by assumptions about the ozone and aerosol profiles used to calculate the two path light extinction, by inaccuracies in the measured temperature/pressure profile or the use of a standard atmosphere, and by uncertainties inherent in determining an aerosol free region for normalization, errors for a lidar system result from signal induced noise and from detector non-linearity for analog detection systems or pulse pileup for photon counting systems. For volcanic conditions there is a large aerosol signal, well above the molecular signal, resulting in small errors. For quiescent conditions this is not the case, typical values of R in quiescent conditions are < 1.05, an aerosol signal which is only < 5% of molecular scattering. To improve the signal in quiescent conditions integration times are increased.

The four lidar records included here are the only multi-decadal lidar records available. They are based at São José dos Campos, Brazil (23.2°S), Mauna Loa, Hawaii (19.5°N),. Hampton, Virginia (37.1°N), and Garmisch-Partenkirchen, Germany (47.5°N). To reduce variations in the measurements due to variations in altitude and thickness of the aerosol layer, the quantity used for long time series comparisons is the vertically integrated backscatter coefficient with units of sr^{-1}. Each lidar will primarily be compared to its own record to assess changes during background periods, but for interest the two tropical and mid latitude lidars will also be compared to each other.

The São José dos Campos (23.2°S, 45.9°W)) measurements use the sodium D2 line at 589 nm and began in 1972. The primary focus of these measurements has been on the atmospheric sodium layer; however, measurements of the stratospheric aerosol content are also available (Clemesha and Simonich, 1978; Simonich and Clemesha, 1997). The wavelength used for the measurements has not changed during the period, although there have been major changes in the laser and improvements in the electronics The measurements presented here represent monthly averages of integrated aerosol backscatter from 17 to 35 km. Error estimates on the integrated profiles are 5%. Since this site is in the tropics, tropopause height fluctuations and variations in the atmospheric density profile are minor. The molecular density profile used is an annual average derived from rawinsonde measurements and TOVS satellite data.

The Mauna Loa, Hawaii (19.5°N) measurements using a ruby laser, 694 nm, began in 1974 with the main focus on stratospheric aerosol [DeFoor et al., 1992; Barnes and Hofmann, 1997; 2001]. In 1994 a new lidar was built using a Nd:YAG laser measuring backscatter at both the 532 nm harmonic and the 1064 nm fundamental. For data continuity the 532 nm data are converted to 694 nm for easy comparison with the early measurements. Errors on the integrated backscatter

range from 15 to > 30% for the ruby measurements, depending on aerosol load. These errors are reduced to approximately 6% for the 532 nm measurements. Since this is another tropical station tropopause fluctuations are minor and the altitude interval for backscatter calculation can be fixed. In this case it is 15.8 to 33 km. Molecular density was obtained from a model for the Ruby lidar analysis and from the nearest radiosonde site (Hilo, Hawaii) for the Nd:YAG lidar. There was an overlapping period of about a year (40 observations) during which the ruby lidar backscatter and the Nd:YAG lidar backscatter at both wavelengths were measured. The average absolute backscatter of the ruby lidar agreed to within 2% of the Nd:YAG backscatter interpolated from the two wavelengths.

The Hampton, Virginia (37.1 N), measurements also use a ruby laser, began in 1974, and are focused on stratospheric aerosol [Fuller et al., 1988; Woods et al., 1994; Osborn et al., 1995]. Although there have been incremental improvements in the system, the fundamental operating wavelength and measurements principles have not changed. For this mid latitude station the integration interval is from the tropopause to 30 km. Errors range from 15 - 50% during stratospheric background periods reducing to 5% for measurements following large eruptions. Molecular densities are obtained from a radiosonde station 120 km to the northeast.

The Garmisch-Partenkirchen, Germany (47.5°N) measurements began in 1976 with a ruby laser and are also focused on stratospheric aerosol [Reiter et al., 1979; Jäger, 1991]. In 1990 to 1991 there was an interruption in the measurements to convert the lidar to a Nd:YAG system. Measurements beginning in 1991 use the 532 nm harmonic of the Nd:YAG laser. As in the case of Mauna Loa, all 532 nm measurements are converted to 694 nm to easily compare with the earlier measurements. Backscatter integrations cover the altitude range, tropopause + 1 km to profile top. Error estimates range from 10 to 50%, depending on stratospheric aerosol load, for the ruby measurements. These errors are reduced by about half for the 532 nm measurements. Molecular density is obtained from a radiosonde station at Munich, 100 km to the north.

c) Remote satellite measurements

The first satellite based aerosol measurement was completed in 1975 using a handheld photometer pointed at the sun as the earth's limb passed over the sun during satellite sunset [Pepin et al., 1977]. This led to the first regular satellite measurements of stratospheric aerosol using a single wavelength photometer measuring solar extinction during 15 sunrises and sunsets by the satellite per day, SAM II [McCormick et al., 1979; 1981; Russell et al., 1981]. The multiwavelength SAGE and SAGE II instruments [Mauldin et al., 1985] followed close behind. These instruments are essentially self calibrating since prior to or after each solar occultation the photometer measures the direct solar transmission without atmospheric extinction. Thus the measured extinction through the atmosphere is truly relative to the solar transmission with all instrument artifacts removed. Converting the measured extinction to an aerosol extinction requires accounting for Rayleigh scatter from the atmosphere as well as specific contributions by molecules with large extinction cross sections at the wavelengths measured. SAM II was a single wavelength instrument measuring aerosol extinction at 1020 nm. SAGE II measures three wavelengths appropriate for measuring O_3, NO_2, and H_2O, and four wavelengths for aerosol extinction.. The inversion of the SAGE II data to provide aerosol extinction is described by [Chu et al., 1989]; and there has been a number of efforts aimed at validating the aerosol extinctions measured [Russell et al., 1984; Oberbeck et al., 1989; Russell and McCormick, 1989]. As the understanding of the instrument

performance has evolved a number of revisions of the SAGE II data have been provided; however, for our purposes the revisions are not critical. For any one revision the same data inversion is applied to all past measurements, thus the relative values of extinction over a 20 year period will stay the same even though the absolute values may change from one revision to another.

Of the eleven instruments deployed on satellites in the past 30 years which include stratospheric aerosol measurements, SAM II, SAGE, SAGE II, SAGE III, Cryogenic Limb Array Etalon Spectrometer (CLAES), HALogen Occultation Experiment (HALOE), and Improved Limb Atmospheric Spectrometer (ILAS), Improved Startsopheric and Mesospheric Sounder (ISAMS), Polar Ozone and Aerosol Monitor (POAM), POAM II, POAM III, only SAM II and SAGE II have records extensive enough to include in this study. SAM II provided high latitude aerosol extinction measurements at 1000 nm from 1979 to 1991, with intermittent measurements extending to 1993 [Poole and Pitts, 1994]. SAGE II has provided aerosol extinction measurements at 386, 452, 525, and 1020 nm from 1984 to 2001 [e.g. Thomason et al., 1997; Hervig and Deshler, 2002]. Of the other satellite instruments HALOE has the longest record reporting aerosol extinction at infrared wavelengths since 1991. Errors for the SAM II and SAGE II measurements are estimated to be 20 to 30% based on a number of comparisons with correlative measurements [Oberbeck et al., 1989; Osborn et al., 1989; Russell and McCormick, 1989]. For SAGE II the difference with correlative measurements was found to be wavelength dependent, with the least difference observed for the 1020 nm measurement.

3. Measurements

For the quantitative comparison of volcanically quiescent periods, the primary measurement from each instrument will be used. The measurements have been checked to be cloud and tropospheric aerosol free and are at latitudes < 50°, thus will not be perturbed by polar stratospheric clouds.

For the in situ measurements approximately monthly profiles of aerosol concentration for particles ≥ 0.15, 0.25 μm are integrated over 5 km columns for the intervals, 15-20, 20-25, and 25-30 km. Typical tropopause heights at Laramie are 10-12 km extending to 15 km in the summer. The column integrals from 15-20 and 20-25 km are presented in Figure 1, adapted from Deshler et al. [2003]. As a point of comparison for these northern mid latitude measurements, measurements 1991-2001 from 45°S made with the same instrumentation as at Laramie are included. Also for reference Junge and co-workers original in situ measurements in the late 1950s are shown displaced forward in time by 10 years. These balloon-borne vertical profile measurements only sampled particles at one size, r > 0.15 μm [Chagnon and Junge, 1961]. The final measurements in 2002 and 2003 show striking variations, but suffer from a sampling frequency reduced to once per year. The particularly low measurement in 2002, 20-25 km, was checked carefully and was confirmed by two independent measurements at 0.25 μm. Column integrals between equivalent theta surfaces were also considered for this analysis, but did not show any significant difference to the altitude integrals. The 0.15 μm mixing ratios plateau at similar values at both altitude intervals for the three background periods, while the 0.25

μm measurements show a bit more variation, remaining elevated in 1990 - 1991 compared to 1979 and 1997.

Histories for the integrated backscatter from the tropical and mid latitude lidars are shown in Figure 2. The tropical lidars use an integration beginning at 16-17 km whereas the mid latitude lidars use the tropopause or tropopause + 1 km as a beginning. Integrations extend to above 30 km. Several points should be mentioned. The São José measurements prior to 1975 have been compared to northern hemisphere measurements in the same time period [Clemesha and Simonich, 1978]. The São José 20 km aerosol backscatter, β_a, was about half that measured in the northern hemisphere in 1973 using an airborne lidar operating at nearly the same wavelength [Fernald and Schuster, 1977]. Better agreement was found when β_a from São José was compared with β_a calculated from in situ aerosol measurements at 41°N in the same time period [Pinnick et al., 1976]. From the data displayed in Figure 2 only the Hampton, Virginia, measurements extend into 1974, and these are in general quantitative agreement with the São José measurements. The suggestion from the São José measurements, of the lowest aerosol loading in the record prior to 1975, is not, however, corroborated by the in situ meausrements, Figure 1. This difference may be partly explained if the São José measurements are biased somewhat low due to the detection threshold of the system in use at that time, or if there was a hemispheric difference in aerosol loading in 1974. Clemesha and Simmonich [1978] suggest the Fuego aerosol was delayed appearing in the southern hemisphere until April 1975 due to the inhibition of eddy transport in 1974 by the meridional circulation in northern winter. Even with this inhibition, there is some suggestion of Fuego aerosol at São José in 1973. Although the integrated backscatters are below the post-Fuego period, there is an aerosol increase in late 1973, following the early 1973 Fuego eruption, and again in early 1975, following the late 1974 Fuego eruption, which appears to be the largest of the three eruptions. The São José measurements in the early 1980s, prior to El Chichón, are in agreement with the Mauna Loa measurements. São José shows a smaller peak and faster decay after El Chichón, but similar peak backscatter and slower decay following Pinatubo. São José measurements are slightly elevated in the background period prior to Pinatubo compared to Mauna Loa measurements and to São José measurements in the period following Pinatubo. The similarity of the fluctuations between São José and Mauna Loa in the 1998 - 2002 period is striking. From the Mauna Loa lidar the pre and post Pinatubo periods are similar, although the random variation of the signal in the pre Pinatubo period is considerably reduced compared to post Pinatubo. For the São José measurements the pre- and post-Pinatubo periods are both characterized by significant fluctuations.

The mid latitude lidars are in quite good agreement throughout the record. The peak integrated backscatter following Pinatubo and El Chichón are similar as are the decay rates. Note that the decay of El Chichón is extended by several minor eruptions compared to the decay of Pinatubo. This feature is also apparent in the in situ measurements particularly in the 15-20 km column. Considering the background periods both lidars agree suggesting that the pre El Chichón and post Pinatubo periods are similar where as the pre Pinatubo period is elevated. This again is similar to the in situ measurements particularly for the 0.25 μm measurements between 15 and 20 km. This correspondence between in situ 0.25 μm measurements and integrated lidar backscatter has been noted

before [Jäger and Hofmann, 1991; Hofmann et al., 2003]. This observation prior to Pinatubo was the reason for Hofmann's [1990] estimate of a 5% yr^{-1} increase in sulfur mass between 1979 and 1989.

Column integrals of zonally averaged SAGE II aerosol extinctions at 1020 nm over the period 1984 - 2001 are shown in Figure 3 The data are zonal averages binned in 10° latitude intervals at the Equator, ±20° and ±40°. The base altitude is always above the tropopause to remove any influence of tropospheric aerosol or clouds. These figues show the decaying vocanic signal of El Chichón followed by the strong increase then decay in optical depth following the eruption of Mt Pinatubo.   The absolute levels of the plots decreases with increasing latitude. This is mostly caused by calcuating the optical depth for a constant altitude range. As the tropopause height lowers towards the poles the aerosol layer also descends, effectively lowering the optical depth for the given altitude range. The difference between the Northern and Southern Hemispheres is within the randomn uncertainty which is typically about 20 %. The major exception to this is during the Pinatubo peak where aerosol was still forming and the difference is most liekly explained by stronger transport into the winter hemisphere from the tropics.

4. Comparison of stratospheric aerosol in non volcanic periods (under construction)-
Identifying the volcanically quiescent periods, weight time periods by our confidence in whether we have reached background. Options for identifying background (All of these will be used):

a) Volcanic record (**Sophie has been asked to work on this building on what Amy Stevermer sent us for the appendix.**)

b) Stratospheric temperature and water vapor changes. This topic has been looked at by Don Grainger with help from Bill Randel. Trends in temperature and water vapor have an insignificant effect on stratospheric aerosol size. (Text added and reviewed by Don.)

c) Back ground periods:

   i)   Each investigator of a primary data set will offer their own estimate of the time periods when the stratospheric aerosol was not perturbed by volcanic eruptions. (This was provided and is shown on Figures 1 and 2),

   ii)   Statistical method (objective) - Point when dQ/dt is not significantly different than zero. Q = quantity measured. (**Explanation of this method has been included; however no results of the method applied to these data sest is yet included.**)

d) Uncertainties will be included. Each investigator supplies: statistical and measurement uncertainties (Completed and included in Section 3.)

e) Statistical analysis of the records comparing the quiescent periods (**Not complete - Betsy?**)

a) **Brief discussion and table listing volcanic activity over the past 30 years**.

b) **Assessing the influence of changes in stratospheric temperatures and water vapor on aerosol size and composition**.

The size and composition of stratospheric aerosol can be predicted from thermodynamics, given sulfuric acid mass, water vapor pressure, and temperature [Steele and Hamill, 1981]. Since over the record of long term stratospheric aerosol measurements there have been increases in stratospheric water vapor and decreases in stratospheric temperature, both of which would lead to larger particles, the effects of these changes was estimated to see if they were significant. Since the 1950s there has been approximately a 1% yr^{-1} increase in stratospheric water vapor [Oltmans and Hofmann, 1995; Kley et al., 2000] and approximately a 0.5 K per decade cooling of the lower to middle stratosphere [Ramaswamy et al., 2001]. These changes in water vapor and temperature were used to estimate the fractional change in particle size and composition. The changes were found to be negligible, less than 10^{-5} μm yr^{-1} in size and -0.05% yr^{-1} in composition in the lower to middle stratosphere between 70°S and 70°N. Thus these changes will not affect this comparison of aerosol in volcanically quiescent periods.

c)   Determination of background time periods

Because our interest is in comparing background aerosol levels, periods in the record unperturbed by volcanic intrusions must be identified. The periods can then be examined and combined to evaluate and understand long-term changes. Because of the relatively short record lengths and brief interludes where background levels are assumed to have been reached, only short periodic perturbations, such as seasonal effects may possibly be identified, in the aerosol data. Decadal or longer-term periodicities cannot be identified in this record. Caution must be taken to limit over-interpretation of differences in background periods. The information may be derived from as few as two epochs containing background data (Figure 1b).

The results of a comparison of background periods will depend in large measure on how the periods are specified. While defining background periods is relatively straight forwered, specifying background periods can be fraught with difficulty since: a) most stratospheric volcanic aerosol decay processes display an exponential rather than linear character, b) there can be input from minor eruptions, such as after El Chichón, between major eruptions, c) recent history has been relatively volcanically active, and d) the time periods for some background periods can be exceedingly short.

Background periods have been identified using multiple methods. We have used two approaches. The first method relies upon the expertise of the investigator responsible for a particular measurement or data set. The researcher, using his or her understanding of the measurement technique and the characteristics of stratospheric aerosol, manually inspects the record and selects time periods that appear to be free of volcanic aerosols. This method is the most subjective, however, it benefits from the investigator's experience in recognizing the effects of volcanic activity. The method relies on a subjective assessment of when the characteristic decay of aerosol mixing ratio, integrated backscatter, or extinction, following a volcanic eruption, no longer influences the record. Some time periods, particularly pre Fuego and pre El Chichón are probably too short to manually determine this unambiguously.

A second common method involves statistical analysis of the data to remove the volcanic periods. This method may as a first step, remove obvious large deviations, which are known to coincide with volcanic eruptions. The resulting data is then analyzed

using various statistical measures to characterize the underlying behavior of that particular series of measurements. This step uses techniques applicable to a wide range of observations and does not necessarily require a priori knowledge of the unique behaviors of a particular aerosol data record. Once the data have been statistically modeled, the model can be used to further trim the data set of points that appear to be outliers. Most of these outlier points will come from the volcanic perturbations, but some points may be removed from background periods, due to their atypical behavior. In addition to helping eliminate volcanic points, this approach will also model the short-term periodic variations in the data. This process can allow seasonal affects to be removed from the background periods, hopefully leaving only the long-term secular signal in the data.

d) **Statistical comparison of the stratospheric aerosol record during volcanically quiescent periods** …

5. Discussion: (under constructions and waiting for trend analysis section)

a) Inherent uncertainties during volcanically quiescent periods. **(This has already been partly addressed in the instrument section.)**

b) Aerosol surface area: Differences between satellite and in situ measurements. (**Completed and published in Deshler et al., JGR, 2003, can also be included here.)**

During periods of low stratospheric aerosol loading measurement precision generally decreases as the aerosol signal decreases. Satellite measurements and in situ measurements are perhaps the least impacted. There is, however, an effect on the retrieval of aerosol surface area from satellite measurements at visible wavelengths [Steele et al., 1999; Deshler et al. 2003]. Typically surface areas and volumes are calculated from visible wavelength extinction measurements using principal component analysis [Twomey, 1977; Thomason and Poole, 1993; Steele et al., 1999]. Figure 4 compares two of the longest records of stratospheric aerosol surface area and volume available [Deshler et al., 2003]. The SAGE II aerosol moments are from the SAGE II data base and are quite similar to results obtained from SAGE II extinctions following Steele et al. [1999]. The SAGE II data are averaged over a $\pm$ 10° longitude and $\pm$ 1° latitude bin centered on Laramie, Wyoming, without any restriction on time. The agreement between the two data sets is well within measurement precision over most of the record. Differences appear primarily during periods of low aerosol loading, with the differences in aerosol surface area greater than the differences in aerosol volume. In low aerosol loading the SAGE II surface areas are centered at the base of the error bars on the Laramie measurements, particularly noticeable since 1997.

A physical explanation for the disparity in surface areas at low aerosol loading is offered in Figure 5. Differential surface area, volume, and extinction distributions are compared for measurements at two altitudes in 1993, under high aerosol loading, and measurements at two altitudes in 1999, under low aerosol loading. At high aerosol loading there is good overlap between the three differential distributions, Figures 5a, b. The median radii of the three distributions, r_s, r_e, r_v, are nearly co-located, particularly at 18 km. At 23 km on 931115 $r_s < r_e$, but there is still excellent overlap of the distributions particularly in the dominant second mode. At low aerosol loading there are significant differences in the median radii and in the sizes covered

13

by the different distributions, Figures 5c, d. In low aerosol loading cases, aerosol surface area is controlled by particles between 0.02 and 0.5 μm, $r_s \sim 0.1$ μm, and ~80% of the total surface area is contributed by particles < 0.15 μm. In contrast the extinction distribution is controlled by particles between 0.05 and 0.5 μm, $r_e \sim 0.2$ μm, and about 25% of the extinction signal is provided by particles less than 0.15 μm. There is less disparity between extinction and volume distributions, although $r_v < r_e$, since the size range spanned by these two distributions is quite similar in both high and low aerosol loading.

Figure 5 suggests that under low aerosol loading the use of extinction measurements to infer aerosol surface area may be problematic, since aerosol surface area is controlled primarily by particles which contribute minimally to extinction. Accurate measurements of aerosol surface areas under clean stratospheric conditions, even from *in situ* measurements, is also uncertain since the dominant mode of the distribution is captured by just a few measurements: CN, and aerosol > 0.15, 0.25 μm. The latter measurements only fix the tail of the distribution and are well above r_s. The size distribution of particles between 0.01 (CN) and r>0.15 μm is calculated using unimdoal lognormal distributions fit to the measurements of the concentration of CN and particles > 0.15 μm. The standard method optimizes the fit to the number concentration measurements with size dependent weighting. A fitting method weighted by surface area produced results which were marginally different than the standard method. A comparison using ~450 measurements split between high and low aerosol loading indicated an increase of 12 ± 36% in surface area for surface area weighted fits to the data compared to no weighting. This result would increase the discrepancy between the in situ and satellite data shown in Figure 4; however, 12% is well within the ± 40% precision associated with the surface area estimates from the in situ measurements [Deshler et al., 2003].

More accurate measurements of surface area requires size resolved concentration measurements between 0.01 and 0.1 μm. Present aircraft instruments are capable of this with size-resolved measurements for particles > 0.03 μm [Jonsson et al., 1995], but resolution of particle sizes below 0.15 μm from balloonborne platforms will have to await instruments now in the planning stage. A partial assessment of the limitations of an OPC, with no size resolution below 0.15 μm, was conducted using stratospheric aircraft measurements from the Focused Cavity Aerosol Spectrometer (FCAS) [Jonsson et al., 1995]. FCAS measurements between 0.03 and 1.67 μm radius in 32 size bins were used to simulate measurements from OPCs sensitive to CN, r>0.01 μm, and particles > 0.15 - 2.0 μm in 12 size bins. Bimodal lognormal distributions were then fit to the simulated OPC measurements and estimated aerosol surface areas were compared to surface areas calculated from the discrete size distributions measured by the FCAS. FCAS measurements from 970923 (20°N - 5°S, θ=380-500K) and 000311 (61-75°N, θ=400-470 K) were used. The lognormal fits to the simulated measurements reproduced the measured size distributions and surface areas reasonably well, Figure 6a; however, there was a systematic overestimation of the surface area by the simulated OPC measurements. Comparisons using ~250 measurements on each day indicated that the fits to the simulated OPC data overestimated sufrace area by 7±15% on 970923 and 26+22% on 000311. The primary source of error was in fitting distributions to the first mode which were too narrow, resulting in under/over estimates of surface area for particles smaller/larger than the median radii, Figure 6b. The overestimation at larger sizes generally overcompensates for under estimatation at smaller sizes. For wider first mode distributions the observations were matched reasonably well and the estimated surface areas were close to the FCAS measurements. Distribution median radii were estimated reasonably well even though the median radii of the first mode was always less than 0.1 μm, well below the first size resolved measurement by the OPC.

A similar comparison of in situ balloon-borne measurements with aerosol surface areas inferred from the Polar Ozone and Aerosol Measurement (POAM) instrument has not been made because of the latitude coverage of the latter instrument; however, a comparison of POAM II, III

and SAGE II aerosol surface areas [Randall et al., 2000; Randall et al., 2001] suggests that a similar discrepancy between *in situ* and POAM estimates of aerosol surface area may exist. The magnitude of the discrepancy, however, may be less, particularly if compared with POAM III which has surface area estimates ~30% greater than SAGE II surface area estimates. POAM II is closer to the SAGE II estimates. Steele et al. [1999] predicted differences in surface areas of this magnitude between the two instruments in background conditions when the aerosol are small.

c) How do current trend results compare with each other, with what is predicted, and with what other published works have shown? What are the sources of any differences? (**Not done.)**

d) What can be learned about aerosol sources, i.e. what does the aerosol burden in background conditions suggest about sulfur sources? (**Obvious overarching scientific question which can be addressed relatively straight forward.)**

e) What is needed for future measurements? (**Obvious necessity to continue the long term records. New measurements to address sources of stratospheric aerosol other than sulfur? Resolution of sizes < 0.1 μm to settle the surface area question.)**

6. Conclusions (waiting for trend analysis and discussion section)

Appendix A --- Major Eruptions during Timeframe of Analysis
Fuego 14.5 N Oct 14 & 17, 1974
Soufriere 13.3 N Apr 14 & 17, 1979
Sierra Negra 0.8 S Nov 13, 1979
St. Helens 46.2 N May 18, 1980
Ulawun 5.0 S Oct 6 & 7, 1980
Alaid 50.8 N April 27-30, 1981
Pagan 18.1 N May 15, 1981
El Chichon 17.0 N Mar 28-Apr 4, 1982
Nevado Del Ruiz 4.9 N Nov 13, 1985
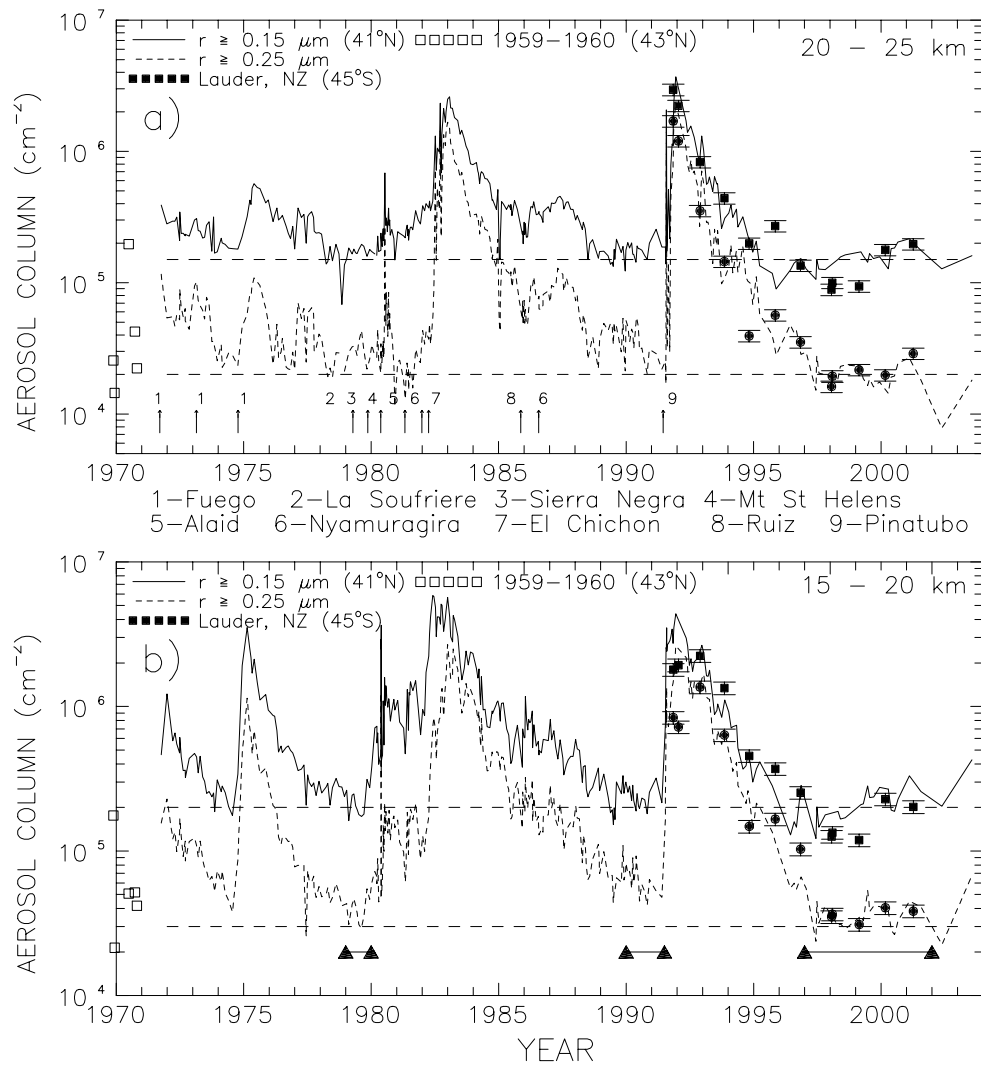Kelut 7.9 S Feb 10, 1990
Pinatubo 15.0 N Jun 12, 1991

Figure 1. History of column integrals of aerosol concentration at 0.15 and 0.25 μm from *in situ* measurements at Laramie, Wyoming, USA (41°N), 1971-2003, and Lauder, New Zealand (45°S), 1991-2001. For reference the results of 5 in situ measurements of aerosol concentration for particles > 0.15 μm made from Sioux Falls, South Dakota 1959-1960, are shown along the left hand axis as open boxes [Chagnon and Junge, 1961]. These measurements are displaced forward in time by 10 years. The Laramie measurements represent about 340 individual aerosol profiles. The error bars on the Lauder measurements are representative of the Laramie measurements as well. a) 20-25 km, b) 15-20 km. The dashed lines are horizontal and are meant only to aid the reader. The regions bounded by triangles in the bottom of b) represent investigator determined background periods. The time and name of the various volcanic eruptions is shown.
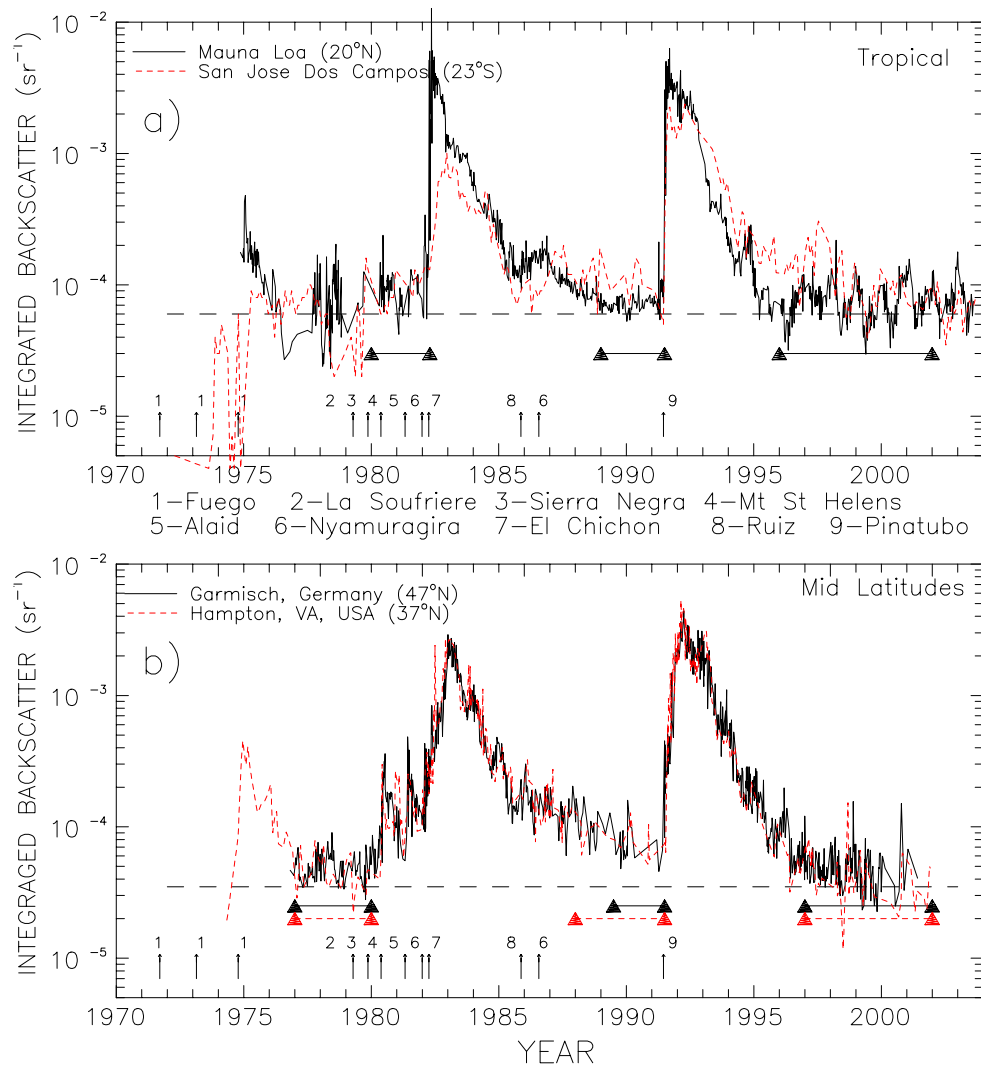
Figure 2. History of integrated backscatter from the tropopause to 30 km from two tropical sites and two mid latitude sites. The wavelengths for all measurements are 694 nm except for São José which is at 589 nm. a) Mauna Loa, Hawaii, USA (20°N), integration from 15.8 - 33 km, and São José dos Campos, Brazil (23°S), integration from 17 - 35 km. b) Garmisch-Partenkirchen, Germany (47°N), integration from tropopause+1 km to layer top, and Hampton, Virginia, USA, integration from tropopause to 30 km. The dashed lines are horizontal and are meant only to aid the reader. The time and name of the various volcanic eruptions is shown. Error estimates range from 5 to 50% and are somewhat dependent on the aerosol load. The regions bounded by triangles in the bottom of a) and b) represent the investigator determined background periods.
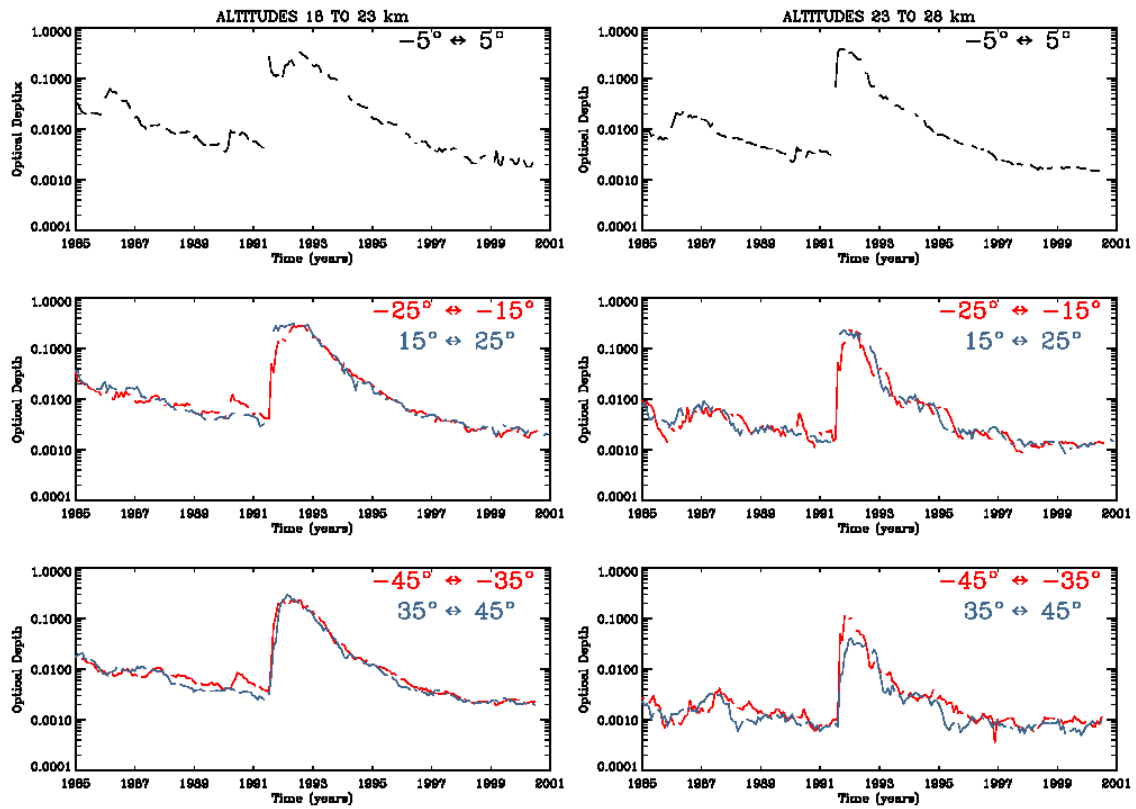
Figure 3. Zonal averages, ± 5°, of SAGE II 1020 nm optical depths versus time centered at 0, ±20 and ±40°. In the the left column the optical depth is caculated between the maximum of 18 km or the tropopause height and 23 km while the in the right hand column the optical depth is caculated for the height range 23-28 km. The blue lines are for the Northern hemisphere and the red for the Southern hemisphere.
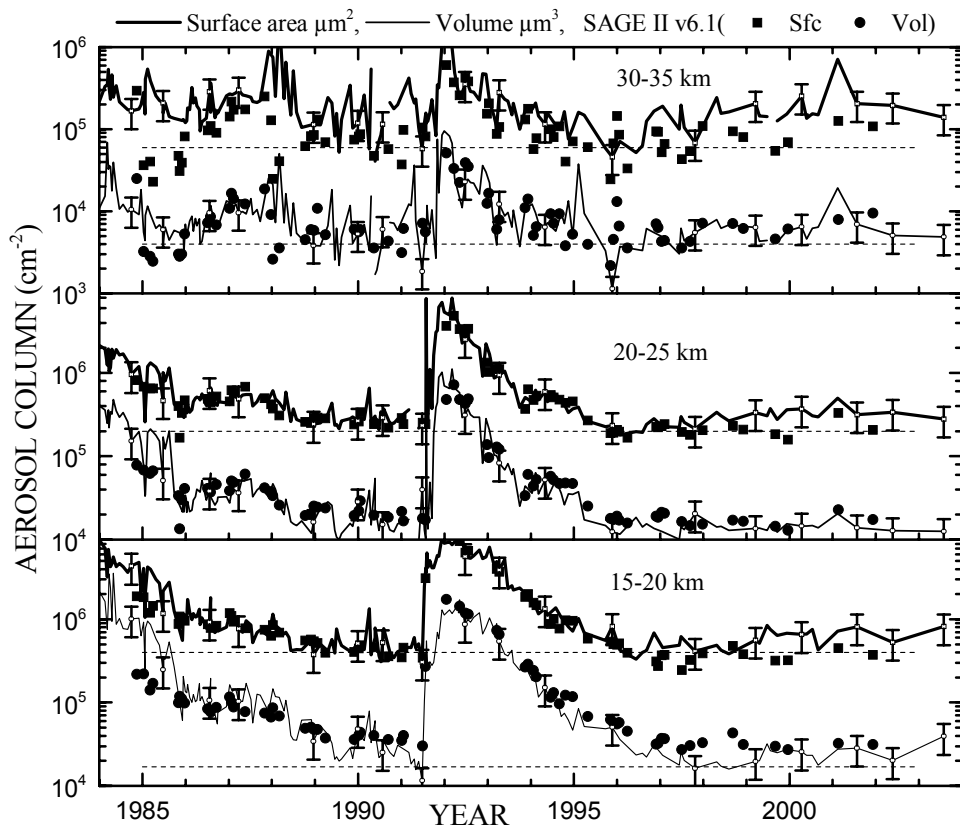
Figure 4. Temporal history of five kilometer column aerosol surface area and volume observed near Laramie, Wyoming, 1984-2004. Solid lines with intermittant error bars (± 40%) are the result of lognormal size distributions fit to ~ 200 aerosol profiles from balloon-borne in situ instruments. The symbols are SAGE II v6.1 estimates of surface area and volume from the SAGE II web site.
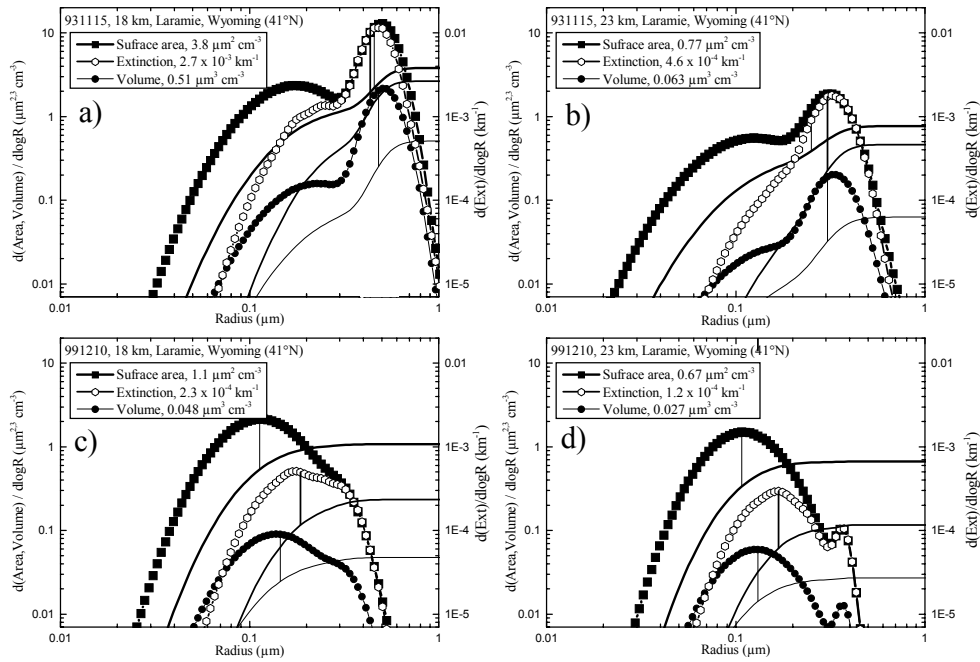
Figure 5. Differential and cumulative distributions of aerosol surface area, volume, and extinction at 525 nm for measurements above Laramie, Wyoming, at two altitudes 18 and 23 km for measurements 1.5 years after Pinatubo, 931115, and at low aerosol loading, 991210. The distributions are derived from in situ measurements of aerosol size distribution. The vertical line connecting the differential and cumulative distributions indicate the distribution median radius, i.e. 50% of the cumulative distribution moment is above and below this size. The values of the integrated distribution moments are shown in the legend.
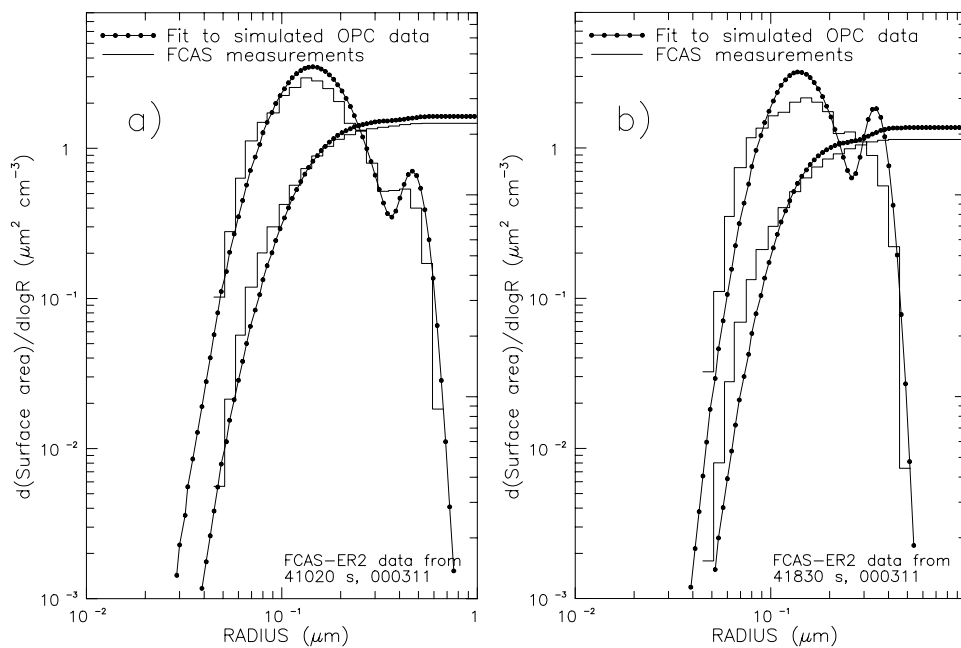
Figure 6. Differential and cumulative surface area distributions from discrete FCAS measurements and from bimodal lognormal distributions fit to simulated OPC measurements derived from the FCAS measurements.

References

Angell, J. K., J. Korshover, and W. G. Planet, Ground-based and satellite evidence for a pronounced total-ozone minimum in early 1983 and responsible atmospheric layers*, Mon. Weather Rev., 113*, 641-646, 1985.

Angell, J. K., Comparisons of stratospheric warming following Agung, El Chichón, and Pinatubo volcanic eruptions, *Geophys. Res. Lett., 20,* 715-718, 1993.

Barnes, J. E., and D. J. Hofmann, Lidar measurements of stratospheric aerosol over Mauna Loa, *Geophys. Res. Lett., 24*, 1923-1926, 1997.

Barnes, J. E., and D. J. Hofmann, Variability in the stratospheric background aerosol over Mauna Loa observatory, *Geophys. Res. Lett., 28*, 2895-2898, 2001.

Chagnon, C. W., and C. E. Junge, The vertical distribution of sub-micron particles in the stratosphere, J. Meteor, 18, 746-752, 1961.

Chu, W. P., M. P. McCormick, J. Lenoble, C. Brogniez, and P. Pruvost, SAGE II inversion algorithm, *J. Geophys. Res., 94*, 8339-8351, 1989.

Clemesha, B. R. and D. M. Simonich, Stratospheric Dust Measurements 1970-1977, *J. Geophys. Res., 83*, 2403-2408, 1978.

Crutzen, P. J., The influence of nitrogen oxide on the atmospheric ozone content*, Q. J. R. Meteorol. Soc., 9*6, 320-327, 1970.

Deshler, T., B. J. Johnson, and W. R. Rozier, Balloonborne measurements of Pinatubo aerosol during 1991 and 1992 at 41°N, vertical profiles, size distribution, and volatility, *Geophys. Res. Lett., 20,* 1435-1438, 1993.

Deshler, T., B. J. Johnson, D. J. Hofmann, and B. Nardi, Correlations between ozone loss and volcanic aerosol at latitudes below 14 km over McMurdo Station, Antarctica, *Geophys. Res. Lett. 23,* 2931-2934, 1996.

Deshler, T., M. E. Hervig, D. J. Hofmann, J. M. Rosen, and J. B. Liley, Thirty years of in situ stratospheric aerosol size distribution measurements from Laramie, Wyoming (41 N), using balloon-borne instruments, *J. Geophys. Res., 108(D5)*, 4167, doi:10.1029/2002JD002514, 2003.

DeFoor, J. E., E. Robinson, and S. Ryan, Early lidar measurements of the June 1991 Pinatubo eruption plume at Manua Loa Observatory, Hawaii, *Geophys. Res. Lett., 19,* 187-190, 1992

Dutton, E. G., and J. R. Christy, Solar radiative forcing at selected locations and evidence for global lower tropospheric cooling following the eruptions of El Chichón and Pinatubo, *Geophys. Res. Lett., 19,* 2313-2316, 1992.

Fahey, D. W., Kawa, S. R., Woodbridge, E. L., Tin, P., Wilson, J. C., Jonsson, H. H., Dye, J. E., Baumgardner, D., Borrmann, S., Toohey, D. W., Avalone, L. M., Proffitt, M. H., Margitan,J., Loewenstein, M., Podolske,J. R., Salawitch, R. J., Wofsy,S. C., Ko, M. K. W., Anderson, D. E., Schoeberl, M. R., Chan, K. K. *In situ* measurements constraining the role of sulphate aerosols in mid-latitude ozone depletion*, Nature, 363, 509-514,* 1993.

Fernald, F. G., and B. G. Schuster, Wintertime 1973 airborne lidar measurements of stratospheric aerosols, *J. Geophys. Res., 82,* 433-437, 1977.

Fiocco G., and G. Grams, Observation of aerosol layer of 20 km by optical radar, *J. Atmos. Sci., 21*, 323-324, 1964.

Fuller, W. H. Jr., M. T. Osborn, and W. H. Hunt, 48-inch lidar aerosol measurements taken at the Langley Research Center: May 1974 to December 1987, NASA RP 1209, October, 1988.

Gleason, J. F., et al., Record low global ozone in 1992, *Science, 260,* 523-526, 1993.

Gruner, P., and H. Kleinert, Die dammerungerscheinen, *Probl. Kosm. Phys., 10*, 1-113, 1927.

Hayashida, S., and M. Horikawa, Anti-correlation between stratospheric aerosol extinction and the Ångström parameter from multiple wavelength measurements with SAGE II - a characteristic of the decay period following major volcanic eruptions, *Geophys. Res. Lett., 19,* 4063-4066, 2001.

Hammer, C. U., H. B. Clausen, and W. Dansgaard, Greenland ice sheet evidence of postglacial volcanism and its climatic impact, *Nature, 288*, 230-235, 1980.

Hansen, J., A. Lacis, R. Ruedy, and K. Sato, Potential climate impact of Mount Pinatubo eruption, *Geophys. Res. Lett., 19*, 215-218, 1992.

Herber, A., L. W. Thomason, V. F. Radinov, and U. Leiter, Comparison of trends in the tropospheric and stratospheric aerosol optical depths in the Antarctic, *J. Geophys. Res., 98*, 18441-18447, 1993.

Hervig, M. E., and T. Deshler, Evaluation of aerosol measurements from SAGE II, HALOE, and balloonborne optical particle counters, *J. Geophys. Res., 107(D3)*, 10.1029/2001JD000703, 2002.

Hofmann, D. J., J. M. Rosen, T. J. Pepin, and R. G. Pinnick, Stratospheric aerosol measurements, I, Time variations at nothern midlatitudes, *J. Atmos. Sci., 32*, 1446-1456, 1975.

Hofmann, D. J. and J. M. Rosen, Stratospheric sulfuric acid layer: Evidence for an anthropogenic component, *Science, 208*, 1368-1370, 1980.

Hofmann, D. J. and J. M. Rosen, On the background stratospheric aerosol layer, *J. Atmos. Sci., 38*, 168-181, 1981.

Hofmann, D. J., and S. Solomon, Ozone destruction through heterogeneous chemistry following the eruption of El Chichón, *J. Geophys. Res., 94,* 5029-5041, 1989.

Hofmann, D. J., Increase in the stratospheric background sulfuric acid aerosol mass in the past 10 years, *Science, 248,* 996-1000, 1990.

Hofmann, D. J. and T. Deshler, Stratospheric cloud observations during formation of the Antarctic ozone hole in 1989, *J. Geophys. Res., 96*, 2897-2912, 1991.

Hofmann, D. J., J. Barnes, E. Dutton, T. Deshler, H. Jäger, R. Keen, and M. Osborn, Surface-based observations of volcanic emissions to the stratosphere, in *Volcanism and the Earth's Atmosphere*, in press, 2003.

Jäger, H. and K. Wege, Stratospheric ozone depletion at northern midlatitudes after major volcanic eruptions, *J. Atmos. Chem., 10*, 273-287, 1990.

Jäger, H. and D. J. Hofmann, Midlatidude lidar backscatter to mass, area, and extinction conversion model based on *in situ* aerosol measurements from 1980 to 1987. Appl. Optics, 30, 127-138, 1991.

Jäger, H., Stratospheric aerosols: Observations, trends, and effects, *J. Aerosol Sci., 22*, suppl. 1, S517-S520, 1991.

Jäger, H., and T. Deshler, Lidar backscatter to extinction, mass and area conversions for stratospheric aerosols based on midlatitude balloonborne size distribution measurements, *Geophys. Res. Lett.,* in press, 2002.

Johnston, P. V., and R. L. McKenzie, NO_2 observatins at 45°S during the decreasing phase of solar cycle 21, from 1980 to 1987, . *J. Geophys. Res., 94*, 3473-3486, 1989.

Johnston, P. V., R. L. McKenzie, J. G. Keys, and W. A. Matthews, Observations of depleted stratospheric NO_2 following the Pinatubo volcanic eruption., *Geophys. Res. Lett., 19,* 211-213, 1992.

Junge, C. E., C. W. Changnon, and J. E. Manson, Stratospheric aerosols, *J. Meteor., 18*, 81-108., 1961.

Junge, C. E., and J. E. Manson, Stratospheric aerosol studies, *J. Geophys. Res., 66*, 3975, 1989

Kley, D., J. M. Russell III, and C. Phillips, *SPARC assessment of upper tropospheric and stratospheric water vapour*, World Climate Research Programme report 113, 2000.

Labitzke, K., and M. P. McCormick, Stratospheric temperature increases due to Pinatubo aerosols, *Geophys. Res. Lett., 19,* 207-210, 1992.

Manabe, S. and R. T. Wetherald, Thermal equilibrium of the atmosphere with a given distribution of relative humidity. *J. Atmos. Sci., 24*, 241-, 1967.

Mauldin, L. E., N. H. Zaun, M. P. McCormick, J. H. Guy, and W. R. Vaughn, Stratospheric Aerosol and Gas Experiment II instrument: A functional description, *Opt. Eng., 24*, 307-312, 1985.

McCormick, M. P., P. Hamill, T. J. Pepin, W. P. Chu, T. J. Swissler, and L. R. McMaster, Satellite studies of the stratospheric aerosol, *Bull. Am. Meteor. Soc., 60*, 1038-1046, 1979.

McCormick, M. P., et al., High-latitude stratospheric aerosols measured by the SAM II satellite system in 1978 and 1979, *Science, 214*, 328-331, 1981.

McCormick, M. P., L. W. Thomason, and C. R. Trepte, Atmospheric effects of the Mt. Pinatubo Eruption, *Nature, 373,* 399, 1995.

Miao, Q., An analysis of errors associated with the measurement of aerosol concentration *in situ* with optical particle counters, M.S. Thesis, University of Wyoming, 71 pp, 2001.

Mozurkiewicz, M., and J. G. Calvert, Reaction probability of N_2O_5 on aqueous aerosols, *J. Geophys. Res., 93*, 15889-15896, 1988.

Oberbeck, V. R., J. M. Libingston, P. B. Russell, R. F. Pueschell, J. M. Rosen, M. T. Osborn, M. A. Kritz, K. G. Snetsinger and G. V. Ferry, SAGE II aerosol validation: Selected altitude measurements, including particle micromeasurements, *J. Geopshy. Res., 94*, 8367-8380, 1989.

Oltmans, S. J., and D. J. Hofmann, Increases in lower-stratospheric water vapor at a mid-latitude northern hemisphere site from 1981 to 1994, *Nature, 374*, 146-149, 1995.

Osborn, M. T., J. M. Rosen, M. P. McCormick, P. Wang, J. M. Livingstion, and T. J. Swissler, SAGE II aerosol correlative observations: Profile measurements, *J. Geopshy. Res., 94*, 8353-8366, 1989.

Osborn, M. T., R. J. DeCoursey, C. R. Trepte, D. M. Winder, and D. C. woods, Evolution of the Pinatubo volcanic cloud over Hampton, Virginia, *Geophys. Res. Lett., 22,* 1101-1104, 1995.

Pepin, T. J., M. P. McCormick, W. P. Chu, F. Simon, T. J. Swissler, R. R. Adams, K. R. Crumbly, and W. H. Fuller, Jr., Stratospheric aerosol measurements, *NASA SP-421*, 127-136, 1977.

Pinnick, R. G., J. M. Rosen, and D. J. Hofmann, Measured light scattering properties of individual aerosol particles compared to Mie scattering theory, *Appl. Optics, 12*, 37-41, 1973.

Pinnick, R. G., and D. J. Hofmann, Efficiency of light-scattering aerosol particle counters, *Appl. Optics, 12*, 2593-2597, 1973.

Pinnick, R. G., J. M. Rosen, and D. J. Hofmann, Stratospheric aerosol measurements III: Optical model calculations. *J. Atmos. Sci., 33*, 304-314, 1976.

Poole, L. R., and M. C. Pitts, Polar stratospheric cloud climatology based on Stratospheric Aerosol Measurement II observations from 1978 to 1989, *J. Geophys. Res., 99,* 13083-13089, 1994.

Prather, M. J., Catastrophic loss of stratospheric ozone in dense volcanic clouds, *J. Geophys. Res., 97,* 10187-10191, 1992.

Pollack, J. B., Toon, O. B. C. Sagan, A. Summers, B. Baldwin, W. V. Camp, Volcanic explosions and climate change: A theoretical assessment, *J. Geophys. Res., 81*, 1071-1083, 1976.

Ramaswamy, V.; Chanin, M.-L.; Angell, J.; Barnett, J.; Gaffen, D.; Gelman, M.; Keckhut, P.; Koshelkov, Y.; Labitzke, K.; Lin, J.-J. R.; O'Neill, A.; Nash, J.; Randel, W.; Rood, R.; Shine, K.; Shiotani, M.; Swinbank, R., Stratospheric temperature trends: observations and model simulations. Rev. Geophysics, 39, 71-122. 2001.

Reiter, R., H. Jäger, W. Carnuth, and W. Funk, The stratospheric aerosol layer observed by lidar since October 1976. A contribution to the problem of hemispheric climate. *Arch. Met. Geoph. Biokl., Ser. B, 27*, 121-149, 1979.

Rosen, J. M., The vertical distribution of dust to 30 km, *J. Geophys. Res., 69,* 4673- 4676, 1964.

Rosen, J. M. and D. J. Hofmann, Optical modeling of stratospheric aerosols: present status, *Appl. Optics, 25*, 410-419, 1986.

Rowland, F. S., H. Sato, H. Khwaja, and S. M. Elliott, The hydrolysis of chlorine nitrate and its possible atmospheric significance, *J. Phys. Chem., 90*, 1985-1988, 1986.

Russell, P.B , and D.Hake, Jr., The post-Fuego stratospheric aerosol: lidar measurements, with radiative and thermal implications, J. Atmos. Sci, 34, 163-177, 1977.

Russell, P. B., M. P. McCormick, T. J. Swissler, W. P. Chu, J. M. Livingston, W. H. Fuller, J. M. Rosen, D. J. Hofmann, L. R. McMaster, D. C. Woods, and T. J. Pepin, Satellite and correlative measurements of the stratospheric aerosol. II: Comparison of measurements made by SAM II, dustsondes, and an airborne lidar, *J. Atmos. Sci., 38*, 1296-1312, 1981.

Russell, P. B., M. P. McCormick, T. J. Swissler, J. M. Rosen, D. J. Hofmann, and L. R. McMaster, Satellite and correlative measurements of the stratospheric aerosol. III: Comparison of measurements made by SAM II, SAGE, dustsondes, filters, impactors, and lidar, *J. Atmos. Sci., 41*, 1792-1800, 1984.

Russell, P. B., and P. Hamill, Spatial variation of stratospheric aerosol acidity and model refractive index: Implications of recent results, *J. Atmos. Sci., 41,* 1781-1790, 1984.

Russell, P. B., and M. P. McCormick, SAGE II aerosol data validation and initial data use: An introduction and overview. *J. Geopshy. Res., 94*, 8335-8338, 1989.

Russell, P. B., J. M. Livingston, E. G. Dutton, R. F. Pueschel, J. A. Reagan, T. E. DeFoor, M. A. Box, D. Allen, P. Pilewskie, B. M. Herman, S. A. Kinne, and D. J. Hofmann, Pinatubo and pre-Pinatubo optical-depth spectra: Mauna Loa measurements, comparisons, inferred particle size distributions, radiative effects, and relationship to lidar data, , *J. Geophys. Res*., *98*, 22969-22985, 1993.

Sato, M., J. E. Hansen, M. P. McCormick, and J. B. Pollack, Stratospheric aerosol optical depths, 1850-1990. , *J. Geophys. Res.*, *98*, 22987-22994, 1993.

Sedlacek, W. A., E. J. Mroz, A. I. Lazrus, and B. W. Gandrud, A decade of stratospheric sulfate measurements compared with observations of volcanic eruptions, *J. Geophys. Res., 88*, 3741-3776, 1983.

Simonich, D. M. and B. R. Clemesha, A History of aerosol measurements at São José dos Campos, Brazil (23 S, 46 W) from 1972 to 1995, *Advances in Atmospheric Remote Sensing with Lidar - Selected papers of the 18. International Laser Radar Conference, Springer-Verlag, Berlin, Germany,* 481-484, 1997.

Solomon, S., R. R. Garcia, F. S. Rowland, and D. J. Wuebbles, On the depletion of Antarctic ozone, *Nature, 321*, 755-758, 1986.

Solomon, S. Stratospheric ozone depletion: A review of concepts and theory, *Rev. Geophys., 37*, 275-316, 1999.

Steele H.M. and P. Hamill, Effect of temperature and humidity on the growth and optical properties of sulfuric acid-water droplets in the Stratosphere, *J. Aerosol Sci., 12*, 517-528, 1981.

Stothers, R. B., Major optical depth perturbations to the stratosphere from volcanic eruptions: Pyrheliometric period, 1881-1960, *J. Geophys. Res.,101*, 3901-3920, 1996.

Swissler, T. J., P. Hamill, M. Osborn, P. B. Russell, and M. P. McCormick, A comparison of lidar and balloon-borne particle counter measurements of the stratospheric aerosol 1974-1980, *J. Atmos. Sci., 39*, 909-916, 1982.

Thomason, L. W., G. S. Kent, C. R. trepte, and L. R. Poole, A comparison of the stratospheric aerosol background periods of 1979 and 1989-1991, *J. Geophys. Res.,102*, 3611-3616, 1997.

Thomason, L. W., L. R. Poole, and T. Deshler, A global climatology of stratospheric aerosol surface area density deduced from stratospheric aerosol and gas experiment II measurements: 1984-1994, *J. Geophys. Res.,102*, 8967-8976, 1997.

Tolbert, M. A., M. J. Rossi, and D. M. Golden, Heterogeneous interactions of chlorine nitrate hydrogen chloride and nitric acid with sulfuric acid surfaces at stratospheric temperatures, *Geophys. Res. Lett., 15*, 847-850, 1988.

Wennberg, P. O., R. C. Cohen, R. M. Stimpfle, J. P. Koplow, J. G. Anderson, R. J. Salawitch, D. W. Fahey, E. L. Woodbridge, E. R. Keim, R. S. Gao, C. R. Webster, R. D. May, D. W. Toohey, L. M. Avallone, M. H. Proffitt, M. Loewenstein, J. R. Podolske, K. R. Chan, and S. C. Wofsy, Removal of stratospheric O_3 by radicals: *In situ* measurements, of OH, HO_2, NO, NO_2, ClO, and BrO, *Science, 266*, 398-404, 1994.

Woods, D. C., M. T. Osborn, D. M. Winker, R. J. DeCoursey, and O. Youngbluth, 48-inch lidar aerosol measurements taken at the Langley Research Center: July 1991 to December 1992, NASA RP 1334, July 1994.

Zhao, R., Laboratory measuerments of the response of optical particle counters to particles of different shape and refractive index, M.S. Thesis, University of Wyoming, 57 pp, 1996.